Level statistics for continuous energy spectra with application to the hydrogen atom in crossed electric and magnetic fields

Gerhard C. Hegerfeldt* and Ralph Henneberg
Institut für Theoretische Physik, University of Göttingen, D-37073 Göttingen, Germany
(Received 29 October 1993)

The statistical analysis of energy levels, a powerful tool in the study of quantum systems, is applicable to discrete spectra. Here we propose an approach to carry level statistics over to continuous energy spectra, paradoxical as this may sound at first. The approach proceeds in three steps, first a discretization of the spectrum by cutoffs, then a statistical analysis of the resulting discrete spectra, and finally a determination of the limit distributions as the cutoffs are removed. In this way the notions of Wigner and Poisson distributions for nearest-neighbor spacing (NNS), usually associated with quantum chaos and regularity, can be carried over to systems with a purely continuous energy spectrum. The approach is demonstrated for the hydrogen atom in perpendicular electric and magnetic fields. This system has a purely continuous energy spectrum from $-\infty$ to ∞. Depending on the field parameters, we find for the NNS a Poisson or a Wigner distribution or a transitional behavior. We also outline how to determine physically relevant resonances in our approach by a stabilization method.

PACS number(s): 32.60.+i, 05.45.+b

I. INTRODUCTION

Statistical properties of the distribution of energy levels have long been recognized as important aspects of quantum systems, in particular for complex nuclei [1,2]. More recently the statistics of nearest-neighbor spacings of energy levels (NNS) has been related to regular and chaotic behavior of trajectories of the corresponding classical system [3]. To allow a statistical comparison of different level spectra these have first to be "rectified" or "unfolded," with normalization to an average of one level per unit interval. It has turned out that for a large number of examples the nearest-neighbor spacings follow a Poisson distribution for classically regular systems and a Wigner distribution for classically chaotic systems. It has therefore been proposed to regard this behavior of the NNS as a tentative criterion for "quantum chaos," whatever sense may be given to this notion, and even regard it as synonymous for it [4].

As a realistic physical system the hydrogen atom in a strong magnetic field has attracted considerable attention and the above ideas have been verified with great numerical accuracy [5,6]. For this system it has also been possible to study the transition between Poisson and Wigner statistics under variation of the field parameter, first in Refs. [7,8] and then in Refs. [9,10], in Ref. [10] with particularly high resolution. In the transition region an interesting resonancelike structure was discovered [9,10], which is associated to a rational value of the classical winding number.

Statistical analysis of energy levels presupposes a discrete or partially discrete level spectrum. It does not apply to a purely continuous energy spectrum, at least not at first sight. We will, however, propose in this paper an approach to carry the statistical analysis over to continuous energy spectra. This at first seemingly paradoxical proposal is based on the following steps.

(i) Initial discretization of spectrum by cutoffs.

(ii) Statistical distributions for the cutoff-dependent discrete spectra.

(iii) Transition to continuous spectrum by removal of cutoff, determination of limit form of distributions.

For such a proposal to work it is essential that the discrete spectra belonging to different cutoffs are rectified in order to treat them on the same footing. Otherwise the limit distributions would just become degenerate.

A simple way of discretizing the energy spectrum consists in replacing the Hilbert space $\mathcal{H}$ of the system by a finite-dimensional subspace $\mathcal{H}_N$, of dimension D_N, and to restrict the Hamiltonian H to this subspace. Denoting by P_N the projection operator onto $\mathcal{H}_N$ this means that one has to diagonalize

$$H_N \equiv P_N H P_N. \tag{1}$$

This becomes effectively a matrix diagonalization. For the eigenvalues of H_N one can, after rectification, determine, for example, the NNS distribution. Then one can increase the cutoff dimension and study the limit behavior of the distributions.

This proposal will now be applied to a hydrogen atom in a magnetic and an electric field which are very strong, constant, and perpendicular to each other. This is a physical system of independent interest. We take the magnetic field $\mathbf{B}$ along the x_3 axis, $\mathbf{B} = (0, 0, B)$, and the

*Electronic address: ghegerf@gwdgv1.dnet.gwdg.de

electric field $\mathbf{F}$ along the x_1 axis, $\mathbf{F} = (F, 0, 0)$. Atomic units are used throughout, so that B and F are measured in multiples of

$$B_0 = 2.35 \times 10^5 \text{ T},$$
$$F_0 = 5.144 \times 10^6 \text{ kV/cm},$$

respectively. These reference fields are very strong compared to available laboratory fields, for which $B, F \ll 1$.

For general vector and scalar potentials the Hamiltonian is, without spin and relativistic effects, of the form

$$H = \frac{1}{2}(\mathbf{p} + \mathbf{A})^2 - \frac{1}{r} + \Phi. \tag{2}$$

In the symmetric gauge this becomes

$$H = \frac{1}{2}\mathbf{p}^2 + \frac{1}{2}BL_3 + \frac{1}{8}B^2(x_1^2 + x_2^2) - \frac{1}{r} + Fx_1, \tag{3}$$

where L_3 is the third component of angular momentum. For both B and F nonzero the only remaining symmetry of H is the reflection π_3 with respect to the x_1-x_2 plane, i.e., the reflection $(x_1, x_2, x_3) \longrightarrow (x_1, x_2, -x_3)$.

For the Zeeman effect, i.e., $F = 0$ and $B \neq 0$, the Hamiltonian in Eq. (3) has infinitely many discrete eigenvalues plus a continuous spectrum [11]. For the Stark effect, i.e., $B = 0$ and $F \neq 0$, the eigenvalue spectrum is purely continuous and extends from $-\infty$ to ∞ [11]. Of more direct physical significance for spectroscopy are the resonances [12], which are complex poles in the resolvent, or Green's function. For electric and magnetic field both *parallel* to the x_3 axis [15] there is rotational symmetry around this axis. The last term in the Hamiltonian in Eq. (3) becomes Fx_3 which commutes with the magnetic field contribution, and therefore one has again the same situation as for the Stark effect with a continuous spectrum from $-\infty$ to ∞.

If $\mathbf{B}$ and $\mathbf{F}$ are *perpendicular* the term $B^2x_1^2/8$ in Eq. (3) dominates Fx_1 when considered as classical potentials, and this might seem to indicate that, as in the Zeeman case, there is both a discrete and a continuous spectrum. This, however, is not so due to the presence of the L_3 term which no longer commutes with the Hamiltonian. One can in fact show rigorously that for both B and F nonzero the Hamiltonian of Eq. (3) has a purely continuous spectrum from $-\infty$ to ∞ [16]. The presence of the $B^2x_1^2/8$ term has, however, a beneficial effect in the numerical treatment, and for this reason we concentrate on the case of perpendicular fields. Also for numerical reasons we confine ourselves to negative energies. The treatment is purely quantum mechanical. It is not the purpose of this paper to present a classical study of this system nor to attempt a comparison with a conceivable semiclassical approach, interesting as this may be. A recent study of this system has been presented in Ref. [17].

In Sec. II we slightly reformulate the eigenvalue problem and explain the analytical setup for the numerical evaluation. The analysis is in terms of the quantity

$$\eta \equiv 1/\sqrt{-2E} \tag{4}$$

and in terms of quantities c_B and c_F, which we call "field parameters," where

$$c_B \equiv \frac{1}{8}\eta^4 B^2, \quad c_F \equiv \eta^3 F. \tag{5}$$

We employ a technically advantageous algebraic approach which has been used by us before [10]. For a particular sequence of finite-dimensional subspaces $\mathcal{H}_N$ and in a judiciously chosen basis the corresponding restricted Hamiltonians H_N become narrow-band matrices whose dimension and number of eigenvalues grow with N. When the $\mathcal{H}_N$'s approach $\mathcal{H}$, the projection operators P_N converge strongly to 1 and therefore one expects $P_N H P_N$ to converge to H in some way. This convergence, and in particular an expected convergence of the discrete spectra to a continuous one, is neither trivial nor obvious. Therefore this question is investigated numerically.

In Sec. III it is demonstrated numerically that prior to rectification of the spectra the number of eigenvalues per unit interval increases with N. The spectra become denser and denser, indicating that they do indeed approach the continuum. This is just what we had expected and it also verifies the continuity of the original spectrum of H.

In Sec. IV the NNS distributions of the rectified spectra are calculated for various cutoffs and for various field parameters. It is shown that for sufficiently high cutoff dimensions the NNS distributions have effectively converged. In this way the limiting NNS distributions are found, and they can be thought of as the NNS distributions for the continuous spectrum. Now one can perform the above mentioned tests for quantum chaos or regularity by looking for Wigner or Poisson distributions or for transition regions. To do this we make a best fit to one of the distributions proposed by Brody [18] for interpolation between Poisson and Wigner distribution and determine the Brody parameter q. This parameter can vary between 0 and 1, corresponding to a Poisson and Wigner distribution, respectively, and we exhibit field parameters for either of them as well as for the transition region. For the corresponding classical system one would expect only chaotic, or only regular trajectories, or a mixture of both, respectively. It would be interesting, but outside the scope of this paper, to check this point for the classical system.

In Sec. V the different, though related, problem of resonances is addressed. In the case of a continuous energy spectrum they are of direct physical significance for spectroscopic measurements and for scattering. For extremely small field parameters they can be calculated by perturbation theory. A semiclassical approach has been investigated by Wintgen [12]. The complex rotation method has recently been used by Main and Wunner [13]; the field parameters considered there are, however, orders of magnitude smaller than those in this paper. To extract information for resonances from our calculations of the discretized spectrum we use a stabilization method [14] which we adapt to our approach. It is interesting and remarkable that this method also seems to work for our extremely high field parameters. Our results may be of practical interest for strong stellar fields.

II. HYDROGEN ATOM IN CROSSED FIELDS

As for the pure magnetic field [10] we find it advantageous also for perpendicular magnetic and electric field to reformulate the Schrödinger equation

$$H\psi_E = E\psi_E \tag{6}$$

for $E < 0$. To this end we introduce the scaling operator U_ζ defined on wave functions by

$$(U_\zeta\psi)(\mathbf{x}) = \zeta\psi(\zeta\mathbf{x}). \tag{7}$$

Because of the factor ζ, instead of $\zeta^{3/2}$, this operator is not unitary in the usual space of square-integrable functions $L^2(\mathbb{R}^3, d^3x)$, but unitary in the space $L^2(\mathbb{R}^3, d^3x/r)$, with a correspondingly modified scalar product. This will be convenient later. We note that

$$\begin{aligned} U_\zeta \mathbf{x} U_\zeta^{-1} &= \zeta\mathbf{x}, \\ U_\zeta \mathbf{p} U_\zeta^{-1} &= \zeta^{-1}\mathbf{p}. \end{aligned} \tag{8}$$

With

$$\eta \equiv 1/\sqrt{-2E}$$

we define

$$\varphi_\eta \equiv U_\eta \psi_E. \tag{9}$$

Multiplying the Schrödinger equation (6) by r and applying U_η one obtains by means of Eq. (8)

$$\{\tfrac{1}{2}r\mathbf{p}^2 + \tfrac{1}{2}r + \tfrac{1}{2}\eta^2 B r L_3 + \tfrac{1}{8}\eta^4 B^2 r(x_1^2 + x_2^2) + \eta^3 F r x_1 - \eta\}\varphi_\eta = 0. \tag{10}$$

Because of the appearance of higher powers of $\eta(E)$ this equation looks at first sight more complicated than the original Schrödinger equation. The numerical advantage, however, is that all operators in this equation are expressible in terms of certain operators L_{ab} most of whose matrix elements vanish. These operators represent the Lie algebra of a so-called dynamical group and are explicitly given in the Appendix.

To transform Eq. (10) to a standard eigenvalue problem we introduce "field parameters" c_B and c_F defined by

$$c_B \equiv \tfrac{1}{8}\eta^4 B^2, \quad c_F \equiv \eta^3 F. \tag{11}$$

Then Eq. (10) becomes

$$\{\tfrac{1}{2}rp + \tfrac{1}{2}r + \sqrt{2c_B}\, r L_3 + c_B r(x_1^2 + x_2^2) + c_F r x_1 - \eta\}\varphi_\eta = 0. \tag{12}$$

Keeping c_B and c_F fixed this becomes a standard eigenvalue problem for η, and therefore this equation now produces spectra not for constant electric and magnetic fields but on curves in the (B, F, E) space as in Fig. 1, given by the relations

$$B = 4\sqrt{2c_B}\mid E \mid, \quad F = c_F(2 \mid E \mid)^{3/2}. \tag{13}$$

The operators in Eq. (12) can now be expressed by the operators L_{ab} from the Appendix, which are self-adjoint on the Hilbert space $L^2(\mathbb{R}^3, d^3x/r)$, i.e., on functions square integrable with respect to d^3x/r and with corresponding scalar product. A convenient basis $\{\mid m, l, n >\}$ in this space is obtained from the usual hydrogen wave functions $\psi_{n,l,m}$ by scaling,

$$\mid m, l, n > \equiv n U_n^{-1} \psi_{n,l,m}\ , \tag{14}$$

where U_n is the U_ζ in Eq. (7) with $\zeta = n$.

A discretization of the spectrum is now achieved by cutting the basis $\{\mid m, l, n >\}$ off at some main quantum number N. The π_3 symmetry of the Hamiltonian splits the basis into two nonmixing parts. We will use the $\pi_3 = 1$ part only, because a factor of 2 in the amount of data gives no great improvement in the statistics computations. To minimize the computational effort we use a particular ordering of the basis elements to obtain a band matrix, with the band of nonzero entries as narrow as possible. We first order with respect to m, then to l, and finally with respect to n. The dimension D_N and bandwidth W_N of the resulting matrix to be diagonalized are

$$\begin{aligned} D_N &= \tfrac{1}{6}\left(N^3 + 3N^2 + 2N\right)\ , \\ W_N &= [\tfrac{1}{2}(N+2)][\tfrac{1}{2}(N+3)]\ , \end{aligned} \tag{15}$$

where the square brackets denote the integral part.

One numerical improvement can still be made for the computations. We can transform Eq. (12) with U_ζ for some constant ζ. This does not change the exact spec-

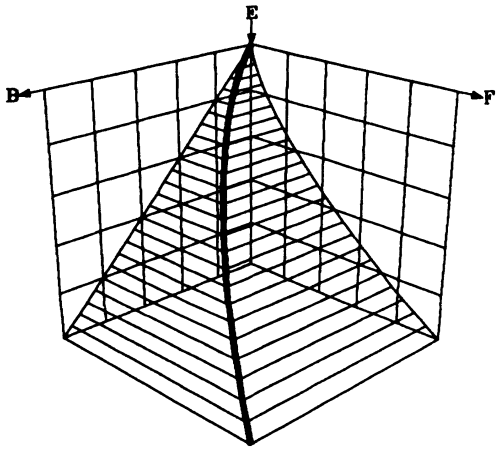

FIG. 1. Curve in B-F-E space corresponding to constant c_B and c_F.

tra because of the unitarity of U_ζ. But the effect on the eigenvalues of the matrices is clearly visible. To decide which ζ to take one could use the mini-max theorem if the Hamiltonian were bounded from below. This theorem states that the highest eigenvalue of the matrix $< \psi_i \mid H \mid \psi_k >$, for $\{\psi_i\}$ orthonormal in an n-dimensional subspace of $\mathcal{H}$, is greater than or equal to the nth eigenvalue of the Hamiltonian. One would therefore call ζ optimal if the highest matrix eigenvalue has a minimum at ζ. Of course this cannot be applied to the case of an electrical field because of the unboundedness of the Hamiltonian from below. But our experience shows that there always exists a value of ζ where many of the matrix eigenvalues go through a minimum as a function of ζ. So the use of this ζ as optimal in the computations seems to be justified.

For our computations we have used field parameters c_B and c_F in the range 0.1–1.6 and basis dimensions up to $D_N = 4060$, corresponding to $N = 28$. For convergence control we have also calculated some particular spectra for $D_N = 5984$, or $N = 32$.

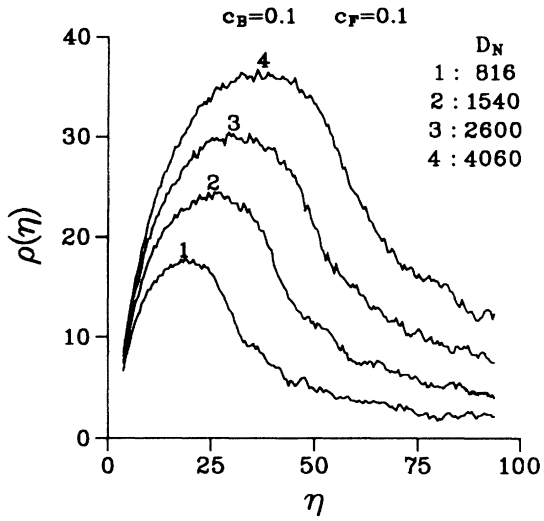

FIG. 2. The eigenvalue density $\rho(\eta)$ is seen to increase for increasing cutoffs ($c_B = 0.1$, $c_F = 0.4$).

III. LEVEL DENSITY: TRANSITION TO CONTINUUM

In this section we determine the behavior of the density of eigenvalues for increasing basis cutoffs N, i.e., for increasing subspace dimension. We intend to verify the expectation that this density increases with dimension. We choose $\eta = \sqrt{-2E}$ instead of E as variable. Picking some interval Δ, small but still sufficiently greater than the mean level spacings, we define the level density $\rho(\eta)$ as

$$\rho(\eta) = \{\text{No. of eigenvalues in } [\eta - \Delta/2, \eta + \Delta/2]\}\,/\Delta.$$

We have calculated this level density and have studied how $\rho(\eta)$ depends on the matrix dimension. We find that indeed for $c_F \neq 0$ the level density becomes larger and larger over the whole range of the spectrum for increasing matrix dimension, indicating that in the limit one obtains a continuum and thus verifying the expectation of the Introduction. A typical example is shown in Fig. 2. Here the field parameters are $c_B = c_F = 0.1$ and the four curves for $\rho(\eta)$ belong to matrix dimensions 816, 1540, 2600, and 4060, corresponding to $N = 16,20,24,28$. The density is clearly seen to grow with dimension. The speed of this depends on η, and it is slow for small η, or large negative energies.

The particular way the level spectra are filled depends strongly on the field parameters. The level densities have a maximum at some value of η and then decrease to 0 for large η, as in Fig. 2. The latter behavior is due to the finiteness of the matrix used for diagonalization. On the other hand, for constant basis dimension the width and position of the maximum depends on the field parameters. Since in Eq. (12) the term quadratic in B is positive an increase of c_B will move the maximum to higher η values and broaden it, as seen in Fig. 3. Increasing c_F has the main effect of moving the maximum to lower η values. This is seen in Fig. 4 where the appearance of negative η's for high c_F values is a numerical artifact resulting from the cutoff, and it diminishes for higher cutoff dimensions.

The accuracy of our computations can be checked for very small values of c_B and c_F, corresponding to laboratory fields, by comparison with a second-order perturbation theory developed by Solov'ev [19]. The agreement is excellent (as far as perturbation theory can reliably be applied) for cutoff dimensions for which the filling of the spectra does not yet show up.

The main conclusion to be drawn from the results of this section is that one can indeed see a transition from a discrete towards a continuous spectrum when increasing the cutoff dimension.

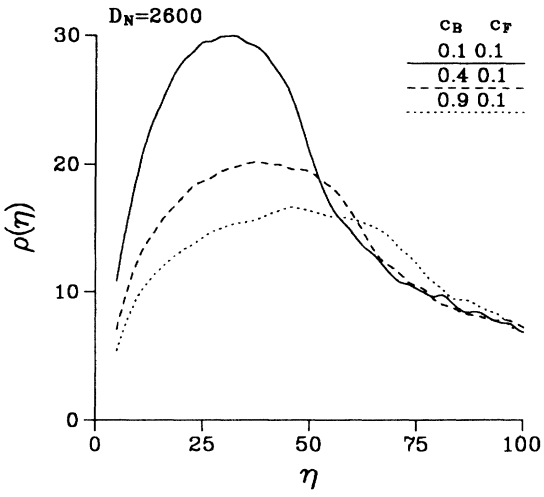

FIG. 3. Eigenvalue density for various values of c_B (fixed cutoff; $c_F = 0.1$).

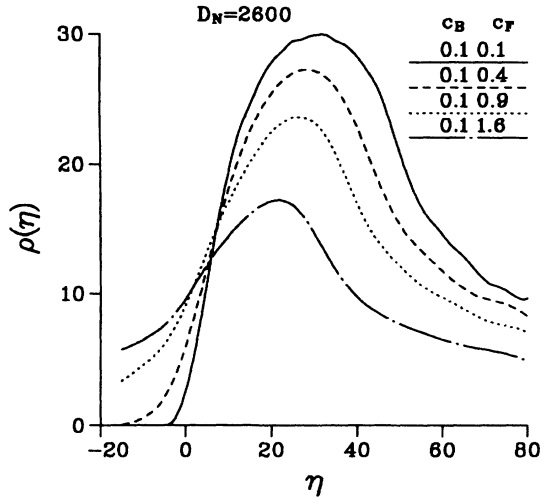

FIG. 4. Eigenvalue density for various values of c_F (fixed cutoff; $c_B = 0.1$).

IV. NNS STATISTICS IN THE LIMIT OF CONTINUOUS SPECTRUM

This section will establish numerical support for our proposal of how to obtain statistical information about a continuous energy spectrum, in particular for NNS statistics. To this end we compute the NNS distributions for the discrete spectra resulting from finite cutoffs and study their behavior as the cutoff becomes larger and larger. Again the analysis will be performed in terms of the η_i's, $\eta_i = \sqrt{-2E_i}$.

One first has to rectify the discrete spectra in order to compare distributions for different cutoffs. This is done in the usual way [20]. The counting function $N(\eta)$ which counts the number of eigenvalues less than η,

$$N(\eta) = \sum_i \Theta(\eta - \eta_i), \tag{16}$$

is interpolated by a smooth function, $\bar{N}(\eta)$ say. With it one can get rid of the global behavior by choosing as new variables e_i instead of η_i, with

$$e_i \equiv \bar{N}(\eta_i). \tag{17}$$

For the resulting spectrum of the e_i's the average number of levels per unit interval is 1. The nearest-neighbor spacings s_i are defined as

$$s_i \equiv e_{i+1} - e_i$$

and their distribution $p(s)$ is defined through

$$\text{Prob}\{\text{some } s_i \text{ in } [s, s+\Delta s]\} = \int_s^{s+\Delta s} p(s)ds. \tag{18}$$

By definition $p(s)$ is normalized and, because the average number of levels per unit interval is 1, the distribution $p(s)$ has mean 1, i.e.,

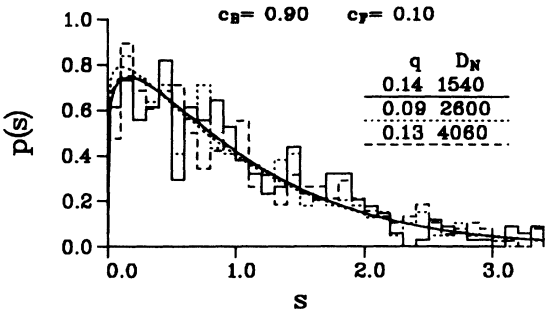

FIG. 5. Convergence of NNS distributions for increasing cutoff. The limit is close to a Poisson distribution.

$$\int_0^\infty sp(s)ds = 1. \tag{19}$$

We have determined the nearest-neighbor distribution $p(s)$ for various field parameters c_B and c_F and have studied its dependence on the cutoff dimension. In Figs. 5 and 6 we have plotted $p(s)$ for the cutoff dimensions 1540, 2600, and 4060, corresponding to $N = 20$, 24, and 28. The full, dotted, and dashed curves are corresponding fits to Brody distributions [21]. It immediately strikes the eye that the curves are hardly distinguishable from each other. The small variation of q by about ± 0.05 has practically no noticeable effect. Thus for these cutoff dimensions the NNS distributions have already essentially converged.

The distribution in Fig. 5 is very close to a Poisson distribution, while the one in Fig. 6 is practically a Wigner distribution, usually associated with quantum chaos.

In principle the Brody parameter q might depend on the spectral window chosen for the statistics. However, the computations show that for a wide range of eigenvalues, which include up to 70% of the spectrum, the Brody parameter is independent of the particular window. The remaining eigenvalues have to be discarded anyway because of boundary effects in the matrix resulting from the finite cutoff dimension.

There exist field parameters representing the whole transition between Poisson and Wigner distribution. In Fig. 7 we have plotted the Brody parameter q as a function of c_B and c_F. For small c_F values q is very small and

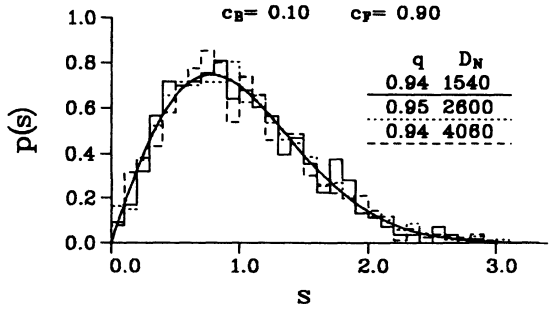

FIG. 6. Convergence of NNS distribution for increasing cutoff. The limit here is close to a Wigner distribution.

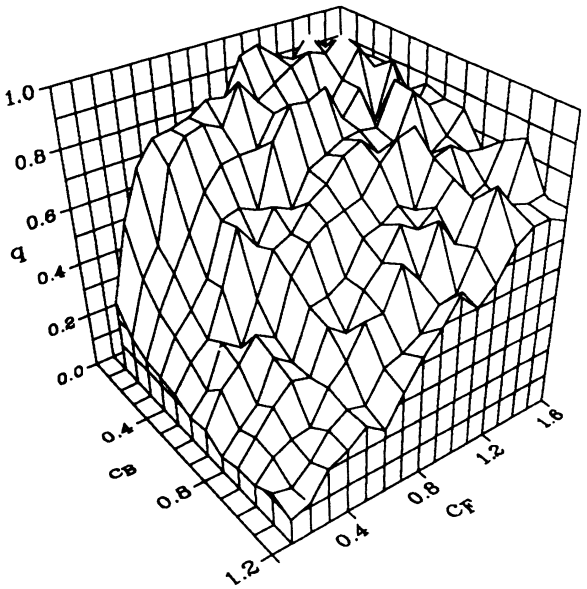

FIG. 7. The Brody parameter q for various values of c_B and c_F. For c_F large the Brody parameter is close to 1 (Wigner distribution).

determines a distribution very close to a Poissonian. At first sight this might seem to contradict the fact that in the pure magnetic field case there is known to be quantum chaos, i.e., $q = 1$. The explanation for this "paradox" is very simple and as follows. For small electric fields the problem is almost symmetric around the x_3 axis, and therefore the magnetic quantum number is approximately a conserved quantity. As a consequence the spectrum consists of a superposition of nearly independent spectra for the various values of m. Such a superposition, however, results in an essentially uniform eigenvalue distribution and hence a Poissonian NNS.

Scaling properties of the classical Hamiltonian [22] would suggest consideration of eigenvalues not on the curves in Fig. 1 for constant c_B and c_F but on curves for which

$$\hat{E} \equiv EB^{-2/3}, \quad \hat{F} \equiv FB^{-4/3}$$

are constant. This will not be done here because the numerical effort for this is much larger and because we do not expect any qualitatively different results.

V. IDENTIFICATION OF RESONANCES

For systems with purely continuous energy eigenvalues the spectrum has in general no direct physical significance but rather the resonances which are associated with poles in the resolvent (Green's operator) and S matrix and with experimentally observed optical spectra [11,23]. In this section we adapt the stabilization method [14] to determine such resonances from our discretized spectra of hydrogen in strong crossed electric and magnetic fields.

As demonstrated in Sec. III the discretized spectra are filled up with increasing cutoff dimension. Moreover, not only do eigenvalue levels appear but the previous ones may change their position. It is a natural question to ask if there are a sort of "stable" eigenvalues which do not change their position or, if so, very little. Because of the increasing eigenvalue density it is impossible to keep track of an individual eigenvalue without some additional label. Such a label can indeed be obtained by not only considering eigenvalues but also eigenvectors. However, with increasing cutoff the eigenvectors lie in different subspaces $\mathcal{H}_N$, and so in turn their identification is not quite trivial. To achieve this we introduce a distance of two normalized vectors by

$$d_{\varphi,\psi} \equiv 1 - |\langle \varphi \mid \psi \rangle|.$$

If the distance is 0 the vectors differ only by a phase factor; if it is 1 they are orthogonal and "far apart." So if we have an eigenvalue with eigenvector $\varphi_{i_0}^{N_1}$ for cutoff N_1 we would, for a higher cutoff, associate it with an eigenvalue whose eigenvector is closest to $\varphi_{i_0}^{N_1}$. Thus we have to know all eigenvectors $\varphi_i^{N_1}$ and $\varphi_j^{N_2}$ and compute their mutual distances

$$1 - |\langle \varphi_i^{N_1}, \varphi_j^{N_2} \rangle|, \tag{20}$$

where P_{N_1} just projects from $\mathcal{H}_{N_2}$ to $\mathcal{H}_{N_1}$. Thus upon increase of the cutoff the eigenvector $\varphi_{i_0}^{N_1}$ turns into an eigenvector $\varphi_{j_0}^{N_2}$ for which

$$|\langle \varphi_{i_0}^{N_1}, \varphi_{j_0}^{N_2} \rangle| = \max_j |\langle \varphi_{i_0}^{N_1}, \varphi_j^{N_2} \rangle|.$$

Our computations have shown that such an association is possible for nearly all eigenvectors. But calculation of eigenvectors requires much more computer time, and so we have restricted ourselves to lower values of the cutoff N.

In Fig. 8 we have drawn narrow vertical columns for various cutoff dimensions and have indicated the corresponding eigenvalues as short horizontal lines in these columns. Between the columns we have connected the eigenvalues by straight lines according to the association outlined above. What immediately strikes the eye is the appearance of quite a number of horizontal straight lines going through the figure. These are the "stable" eigenvalues we have been looking for.

From the study of model systems it has been suggested [14] to identify the "stable" eigenvalues with resonances, or rather with their real parts. In our case we can check this for small fields by comparison with perturbation theory. For the Stark effect it is known that perturbation theory actually yields resonances [11]. For very small field parameters and not too high cutoff dimension all eigenvalues are "stable" in the above sense and agree with the results of perturbation theory. Hence the identification with resonances is justified in this regime.

With this identification of "stable" eigenvalues as resonances we now discuss their qualitative behavior for various field parameters c_B and c_F. Here one has to distinguish the cases of dominating magnetic versus dominating electric field parameter. If c_F is small compared to

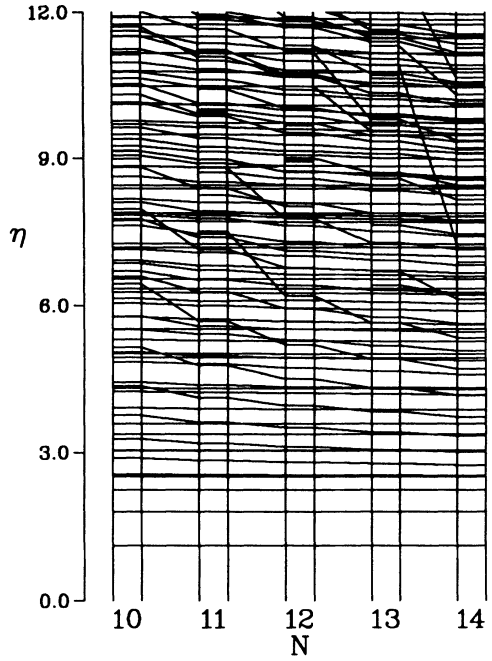

FIG. 8. Identification of stable eigenvalues as horizontal lines for $c_B = 0.1$ and $c_F = 0.1$.

c_B, as in Fig. 8, there are relatively many "stable" eigenvalues. Their number decreases more and more when c_F is larger than c_B. This is seen in Fig. 9 with $c_B = 0.3$ and $c_F = 0.6$ where only few horizontal straight lines are recognizable.

The general situation emerges as follows. For low field

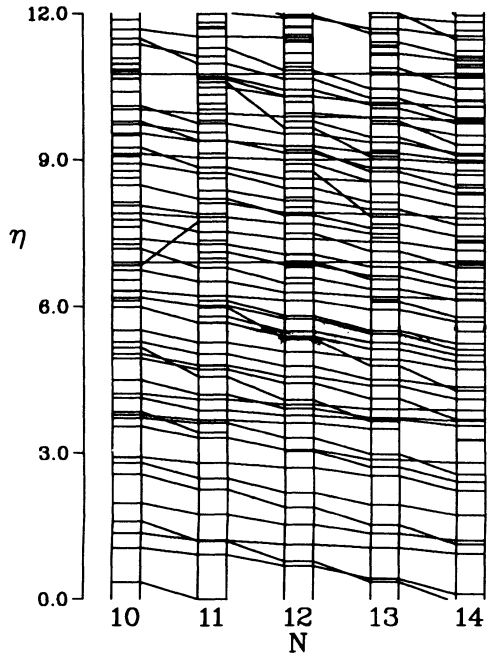

FIG. 9. As in Fig. 8, but with $c_B = 0.3$ and $c_F = 0.6$. For large c_F there are fewer horizontal lines.

parameters one observes a large number of "stable" eigenvalues, which we identify with resonances. Increasing c_F compared to c_B diminishes the number of "stable" eigenvalues (resonances) more and more so that finally for very high c_F the "stable" eigenvalues have vanished completely. This would imply that experimentally observed optical spectra should show less and less structure.

VI. CONCLUSIONS

Statistical analysis of energy levels has been a powerful tool in the study of quantum systems with a discrete energy spectrum, but it seems at first sight not to be applicable to systems with continuous energy eigenvalues only. In the foregoing we have proposed an approach to carry the analysis over to systems with a purely continuous energy spectrum. The main idea has been to first discretize the energy spectrum by some cutoff and then to study the convergence properties of the statistical quantities as the cutoff is removed. If generally applicable, the approach would allow one to extend the study of "quantum chaos" in terms of spectral statistics from discrete levels to continuous spectra.

We have applied this approach to a hydrogen atom in a magnetic and an electric field perpendicular to each other. This system has a purely continuous spectrum of eigenvalues extending from $-\infty$ to ∞. For numerical reasons we have considered the negative part of the spectrum only. We have first discretized the spectrum by a cutoff of the basis, leading to finite-dimensional matrix diagonalizations, and have then demonstrated numerically that the level density increases towards the continuum with increasing dimension. The filling of the spectrum depends on the field strengths, in particular the speed of filling when the dimension is increased. When the magnetic field contribution to the Hamiltonian dominates the electric part the filling is very slow and one has to go to very large bases to see it. This is not unexpected since for the Zeeman effect, i.e., zero electric field, the levels lying in $(-\infty, 0)$ are discrete and bounded from below. For larger electric field the filling is much faster and one can see the appearance of a continuous spectrum, extending to larger and larger negative energies.

We have investigated the statistics of nearest-neighbor spacings and have demonstrated numerically that the NNS distributions converge when the cutoff dimension becomes larger and larger. One should bear in mind that NNS distributions are generally calculated for discrete level spectra which have first been rectified. Otherwise the NNS distributions would of course become degenerate in the limit.

The limiting distributions show an interesting behavior. For small fields one finds Poisson statistics, as expected. But this is true also for larger fields, if only the magnetic field dominates the electric one. This is relatively simple to understand through the superposition of many almost independent spectra and has been explained in Sec. IV. For increasing electric field, however, the distributions get closer and closer to a Wigner distribution. For discrete levels the appearance of a Wigner

distribution is generally regarded as a sign for "quantum chaos." If one accepts carrying this identification over to a continuous spectrum then we have demonstrated the existence of quantum chaos for hydrogen in perpendicular magnetic and electric fields for certain field parameters. It would be interesting to investigate the corresponding classical system and check whether the trajectories become chaotic for these field parameters. But such an investigation is beyond the scope of this paper.

Finally, we have investigated "stable" eigenvalues in a continuous spectrum and, following the ideas of the stabilization method, have identified them as resonances. If correct this would allow a determination of resonances for very strong fields when perturbation theory is not applicable. This might be interesting for strong stellar fields. It might also be used for resonance statistics, as opposed to statistics of energy levels. It is presently not clear what the connection between the two is, if there is any. The above approach might contribute to a clarification of this point. In this context it should be borne in mind that in spectroscopic experiments one usually determines resonances when the energy spectrum is continuous. For the laboratory fields available until now this distinction usually is, and can be, disregarded, since perturbation theory is applicable, and not surprisingly only Poisson statistics has been found for these relatively low fields [24].

We suggest applying our approach also to other systems with a continuous energy spectrum, to check if it works just as well as it does for the hydrogen atom in crossed fields, and to study the connection between statistical properties of continuous eigenvalues with classical trajectories. In this sense our paper poses more questions than it answers, but hopefully it will stimulate further research.

APPENDIX

The unperturbed hydrogen atom can be treated by purely algebraic methods, based on the Lie algebra of the dynamical group so(4,2) [25]. The basis elements of the Lie algebra can be arranged as elements L_{ab} of a 6×6 antisymmetric matrix,

$$(L_{ab}) \equiv \begin{pmatrix} 0 & L_3 & -L_2 & A_1 & B_1 & \Gamma_1 \\ -L_3 & 0 & L_1 & A_2 & B_2 & \Gamma_2 \\ L_2 & -L_1 & 0 & A_3 & B_3 & \Gamma_3 \\ -A_1 & -A_2 & -A_3 & 0 & T_2 & T_1 \\ -B_1 & -B_2 & -B_3 & -T_2 & 0 & T_3 \\ -\Gamma_1 & -\Gamma_2 & -\Gamma_3 & -T_1 & -T_3 & 0 \end{pmatrix}, \tag{A1}$$

which obey the commutation relations

$$[L_{ab}, L_{bc}] = i\epsilon_b L_{ac} , \tag{A2}$$

where $(\epsilon_b) = (-1,-1,-1,-1,+1,+1)$. All remaining commutators vanish. The L_i's are the components of quantum mechanical angular momentum,

$$\mathbf{L} = \mathbf{r} \times \mathbf{p},$$

and the A_i's are defined by

$$\mathbf{A} := \frac{1}{2}\mathbf{r}\mathbf{p}^2 - \mathbf{p}(\mathbf{r}\cdot\mathbf{p}) - \frac{1}{2}\mathbf{r}. \tag{A3}$$

$\mathbf{A}$ can be related to the quantum mechanical Runge-Lenz vector. The six operators L_i, A_i form a basis for the Lie algebra so(4) and describe the degeneracy of the unperturbed hydrogen energy levels.

The three operators T_i are

$$T_1 := \frac{1}{2}(r\mathbf{p}^2 - r), \quad T_2 := \mathbf{r}\cdot\mathbf{p} - i, \quad T_3 := \frac{1}{2}(r\mathbf{p}^2 + r) , \tag{A4}$$

which obey the commutation relations of an so(2,1) algebra,

$$[T_1, T_2] = -iT_3, \quad [T_2, T_3] = iT_1, \quad [T_3, T_1] = iT_2. \tag{A5}$$

The commutation relations in Eq. (A2) then lead to

$$\mathbf{B} = \frac{1}{2}\mathbf{r}\mathbf{p}^2 - \mathbf{p}(\mathbf{r}\cdot\mathbf{p}) + \frac{1}{2}\mathbf{r}, \qquad \mathbf{\Gamma} = r\mathbf{p}. \tag{A6}$$

Not all of these operators are Hermitian in the usual Hilbert space $L^2(\mathbb{R}^3, d^3x)$ of square-integrable functions, but they become Hermitian in the space $L^2(\mathbb{R}^3, d^3x/r)$ with the measure d^3x/r instead of the usual d^3x. An orthonormal basis in this space is

$$|\, m,l,n\rangle \equiv N_{nl} e^{-r}(2r)^l L^{2l+1}_{n-l-1}(2r) Y_{lm}(\theta,\phi). \tag{A7}$$

These can be obtained from the usual hydrogen eigenfunctions by a scale transformation nU_n^{-1} where U_n is given by Eq. (7). The labeling quantum numbers are thus in the range $m = -l,\ldots,l$, $l = 0,\ldots,n-1$, and $n = 1,2,\ldots$. The actions of some of the so(4,2) operators on these basis vectors are given by

$$\begin{aligned}
L_3\,|\,n,l,m\rangle &= m\,|\,n,l,m\rangle , \\
\mathbf{L}^2\,|\,n,l,m\rangle &= l(l+1)\,|\,n,l,m\rangle , \\
L_\pm\,|\,n,l,m\rangle &= \sqrt{l(l+1)-m(m\pm1)}\,|\,n,l,m\pm1\rangle , \\
T_3\,|\,n,l,m\rangle &= n\,|\,n,l,m\rangle , \\
\mathbf{T}^2\,|\,n,l,m\rangle &= l(l+1)\,|\,n,l,m\rangle , \\
T_\pm\,|\,n,l,m\rangle &= \sqrt{n(n\pm1)-l(l+1)}\,|\,n\pm1,l,m\rangle , \\
A_3\,|\,n,l,m\rangle &= c_{n,l}\sqrt{l^2-m^2}\,|\,n,l-1,m\rangle - c_{n,l+1}\sqrt{(l+1)^2-m^2}\,|\,n,l+1,m\rangle , \\
A_\pm\,|\,n,l,m\rangle &= \pm c_{n,l}\sqrt{(l\mp m)(l\mp m-1)}\,|\,n,l-1,m\pm1\rangle \mp c_{n,l+1}\sqrt{(l\pm m+1)(l\pm m+2)}\,|\,n,l+1,m\pm1\rangle ,
\end{aligned}$$

where $c_{n,0} = 0$ and

$$c_{n,l} = \sqrt{\frac{n^2 - l^2}{4l^2 - 1}}.$$

These operators also allow the calculation of matrix elements for various combinations of space and momentum operators by using their definitions and commutation relations. In particular one has

$$x_i = B_i - A_i, \quad r = T_3 - T_1, \quad r\mathbf{p}^2 = T_1 + T_3, \tag{A8}$$

and from this one finds rL_3. The action of $r(X_1^2 + x_2^2)$ and rx_1 on a basis vector, needed in Eq. (7), yields linear combinations of 21 and 20 basis vectors, respectively. These combinations can be calculated by the computer language REDUCE to avoid misprints frequently occurring in the literature.

[1] N. Rosenzweig, Phys. Rev. Lett. **1**, 24 (1958).

[2] Cf. also the review article by O. Bohigas in *Chaos and Quantum Physics,* Les Houches, Session LII, edited by M.-J. Giannoni, A. Voros, and I. Zinn-Justin (North-Holland, Amsterdam, 1991), p. 87, and references therein.

[3] M. V. Berry and M. Tabor, Proc. R. Soc. London **356**, 375 (1977); O. Bohigas, M. J. Giannoni, and C. Schmit, Phys. Rev. Lett. **52**, 1 (1984); G. Casati, B. V. Chirikov, and I. Guarneri, *ibid.* **54**, 1350 (1985); **56**, 2768 (1986); T. Zimmermann, H.-D. Meyer, H. Köppel, and L. S. Cederbaum, Phys. Rev. **A 33**, 4334 (1986); H. Frahm and H. J. Mikeska, Z. Phys. **B 60**, 117 (1985); **65**, 249 (1986); in *Quantum Chaos and Statistical Nuclear Physics*, edited by T. H. Seligman and H. Nishioka, Lecture Notes in Physics Vol. 263 (Springer-Verlag, Berlin, 1986).

[4] There are also quantum manifestations of chaos in scattering theory. Cf., e.g., M. C. Gutzwiller, Physica D **7**, 341 (1983); *Chaos in Classical and Quantum Mechanics* (Springer, New York, 1990); U. Smilansky in Ref. [2], p. 371, and references therein.

[5] D. Wintgen and H. Friedrich, Phys. Rev. Lett. **57**, 571 (1986); J. Phys. B **19**, 991 (1986).

[6] D. Delande and J. C. Gay, Phys. Rev. Lett. **57**, 2006 (1986); **59**, 1809 (1987).

[7] G. Wunner, U. Woelk, I. Zech, G. Zeller, T. Ertl, F. Geyer, W. Schweitzer, and H. Ruder, Phys. Rev. Lett. **57**, 3261 (1986).

[8] D. Wintgen and H. Friedrich, Phys. Rev. **A 35**, 1464 (1987).

[9] A. Hönig and D. Wintgen, Phys. Rev. **A 39**, 5642 (1989).

[10] G. C. Hegerfeldt and R. Henneberg, Phys. Rev. **A 41**, 1161 (1990).

[11] W. Thirring, *Lehrbuch der mathematischen Physik, Band 3: Quantenmechanik der Atome und Moleküle* (Springer, Berlin, 1979).

[12] D. Wintgen, J. Phys. B **22**, L5 (1989).

[13] J. Main and G. Wunner, Phys. Rev. Lett. **69**, 586 (1992).

[14] V. A. Mandelshtam, T. R. Ravuri, and H. S. Taylor, Phys. Rev. Lett. **70**, 1932 (1993); A. U. Hazi and H. S. Taylor, Phys. Rev. A **1**, 1109 (1970); I. Eliezer, H. S. Taylor, and J. K. Williams, J. Chem. Phys. **47**, 2165 (1967).

[15] K. Richter, D. Wintgen, and J. S. Briggs, J. Phys. B **20**, L627 (1987).

[16] K. Jörgens, Math. Z. **96**, 355 (1967), has studied the spectra of Schrödinger operators in great generality. The general result in his Theorem (7.1) can be specialized to the case at hand by regarding $1/r$ as a perturbation.

[17] G. Raithel, M. Fauth, and H. Walther, Phys. Rev. A **47**, 419 (1993).

[18] T. A. Brody, Lett. Nuovo Cimento **7**, 482 (1973).

[19] E. A. Solov'ev, Zh. Eksp. Teor. Fiz. **82**, 1762 (1982) [Sov. Phys. JETP **55**, 1017 (1982)]; **85**, 109 (1983) [**58**, 63 (1983)]; P. A. Braun and E. A. Solov'ev, *ibid.* **86**, 68 (1984) [*ibid.* **59**, 38 (1984)]. The second-order perturbation theory developed there can easily be adapted to the curves corresponding to constant c_B and c_F values considered here.

[20] See, e.g., D. Delande, Ref. [2], p. 665.

[21] The Brody distributions [18] which interpolate between Poisson and Wigner distributions are given by

$$p_q(s) = As^q \exp\{-\alpha s^{q+1}\},$$

with

$$\alpha = \left[\Gamma\left(\frac{q+2}{q+1}\right)\right]^{q+1} \quad \text{and} \quad A = (q+1)\alpha.$$

For $q = 0$ and $q = 1$ this becomes the Poisson and Wigner distribution, respectively,

$$p_P(s) = e^{-s},$$
$$p_W(s) = \frac{1}{2}\pi e^{-\pi s^2/2}.$$

Though introduced phenomenologically, the Brody distributions are better adapted to level repulsion, i.e., to $p(0) = 0$, than the more physically motivated interpolation proposed by M. V. Berry and M. Robnik, J. Phys. A **17**, 2413 (1984).

[22] A. Harada and H. Hasegawa, J. Phys. A **16**, L259 (1984).

[23] I. W. Herbst and B. Simon, Phys. Rev. Lett. **41**, 67 (1978), and references therein.

[24] G. Wiebusch, J. Main, K. Krüger, H. Rottke, A. Holle, and K. H. Welge, Phys. Rev. Lett. **62**, 2821 (1989).

[25] A. O. Barut and H. Kleinert, Phys. Rev. **156**, 1541 (1967): A. O. Barut, *Dynamical Groups and Generalized Symmetries in Quantum Theory* (University of Canterbury Publications, Christchurch, 1972); A. Bohm, *Quantum Mechanics: Foundations and Applications*, 2nd ed. (Springer, New York, 1986). It should be noted that D. Delande and J. C. Gay [6] use a two-oscillator approach which leads to a different operator realization of so(4,2).